AMERICAN SOCIETY FOR MICROBIOLOGY | Applied and Environmental Microbiology®

BIOTECHNOLOGY

Exposure to UV-B Radiation Leads to Increased Deposition of Cell Wall-Associated Xerocomic Acid in Cultures of *Serpula himantioides*

Solange Torres,[a] Mariela González-Ramírez,[a] Javiera Gavilán,[b] Cristian Paz,[c] Goetz Palfner,[a] Norbert Arnold,[d] Jorge Fuentealba,[b] José Becerra,[a] Claudia Pérez,[a] Jaime R. Cabrera-Pardo[a,e]

[a]Departamento de Botánica, Facultad de Ciencias Naturales y Oceanográficas, Universidad de Concepción, Concepción, Chile
[b]Departamento de Fisiología, Facultad de Ciencias Biológicas, Universidad de Concepción, Concepción, Chile
[c]Departamento de Ciencias Básicas, Universidad de La Frontera, Temuco, Chile
[d]Department of Bioorganic Chemistry, Leibniz Institute of Plant Biochemistry, Halle, Germany
[e]Departamento de Química, Facultad de Ciencias, Universidad del Bio-Bio, Concepción, Chile

ABSTRACT Many fungi are thought to have developed morphological and physiological adaptations to cope with exposure to UV-B radiation, but in most species, such responses and their protective effects have not been explored. Here, we study the adaptive response to UV-B radiation in the widespread, saprotrophic fungus *Serpula himantioides*, frequently found colonizing coniferous wood in nature. We report the morphological and chemical responses of *S. himantioides* to controlled intensities of UV-B radiation, under *in vitro* culture conditions. Ultraviolet radiation induced a decrease in the growth rate of *S. himantioides* but did not cause gross morphological changes. Instead, we observed accumulation of pigments near the cell wall with increasing intensities of UV-B radiation. Nuclear magnetic resonance (NMR) and high-performance liquid chromatography-mass spectrometry (HPLC-MS) analyses revealed that xerocomic acid was the main pigment present, both before and after UV-B exposure, increasing from 7 mg/liter to 15 mg/liter after exposure. We show that xerocomic acid is a photoprotective metabolite with strong antioxidant abilities, as evidenced by DPPH (2,2-diphenyl-1-picrylhydrazyl), ABTS [2,2′-azino-bis(3-ethylbenzothiazoline-6-sulfonic acid) diammonium salt], and oxygen radical absorbance capacity (ORAC) assays. Finally, we assessed the capacity of xerocomic acid as a photoprotective agent on HEK293 cells and observed better photoprotective properties than those of β-carotene. Xerocomic acid is therefore a promising natural product for development as a UV-protective ingredient in cosmetic and pharmaceutical products.

IMPORTANCE Our study shows the morphological and chemical responses of *S. himantioides* to controlled doses of UV-B radiation under *in vitro* culture conditions. We found that increased biosynthesis of xerocomic acid was the main strategy adopted by *S. himantioides* against UV-B radiation. Xerocomic acid showed strong antioxidant and photoprotective abilities, which has not previously been reported. Our results indicate that upon UV-B exposure, *S. himantioides* decreases its hyphal growth rate and uses this energy instead to increase the biosynthesis of xerocomic acid, which is allocated near the cell wall. This metabolic switch likely allows xerocomic acid to efficiently defend *S. himantioides* from UV radiation through its antioxidant and photoprotective properties. The findings further suggest that xerocomic acid is a promising candidate for development as a cosmetic ingredient to protect against UV radiation and should therefore be investigated in depth in the near future both *in vitro* and *in vivo*.

KEYWORDS pigments, *Serpula himantioides*, UV-B radiation, xerocomic acid

Citation Torres S, González-Ramírez M, Gavilán J, Paz C, Palfner G, Arnold N, Fuentealba J, Becerra J, Pérez C, Cabrera-Pardo JR. 2019. Exposure to UV-B radiation leads to increased deposition of cell wall-associated xerocomic acid in cultures of *Serpula himantioides*. Appl Environ Microbiol 85:e00870-19. https://doi.org/10.1128/AEM.00870-19.

Editor Irina S. Druzhinina, Nanjing Agricultural University

Address correspondence to Claudia Pérez, claudiaperez@udec.cl, or Jaime R. Cabrera-Pardo, jacabrera@ubiobio.cl.

Received 15 April 2019
Accepted 27 June 2019
Accepted manuscript posted online 8 July 2019
Published 29 August 2019

The continuous depletion of stratospheric ozone has led to a substantial increase in UV-B radiation (UV-B) on Earth's surface. As this harmful abiotic stress reaches our planet in increasing levels, it has the potential to cause irreversible damage to biological systems (1). A direct consequence of UV-B to living organisms is the generation of reactive oxygen species (ROS), which are highly reactive chemical entities that can cause serious injury to cellular structures. This negative effect is mainly caused by UV-B, which leads to DNA damage by generating different types of mutagenic lesions (2–5). However, some living organisms have developed efficient metabolic pathways to synthesize chemical moieties, such as pigments, which are able to cope with this harmful energy, and reactive radicals to provide protection against UV radiation (6–11).

Fungi represent one of the largest groups of organisms and are widely distributed across both mild and extreme ecosystems on our planet (12). They show a unique metabolic plasticity that has allowed them to rapidly adapt and survive through the biosynthesis of a wide array of natural products (13). Despite the great ability of fungi to produce structurally diverse compounds, the study of their chemical response upon exposure to UV radiation has been limited to a small number of species, largely unicellular and filamentous fungi (14–17). Previous studies in these organisms have shown that UV radiation has detrimental effects on germination, sporulation, and colony diameter. In *Aspergillus carbonarius* and *Aspergillus parasiticus*, for example, UV radiation had a significant effect on the size, diameter, and density of the colonies as well as biomass dry weight (18). In a study involving *Penicillium italicum*, all UV-B intensities examined had inhibitory effects on *in vitro* growth, showing a reduction of spore germination of over 99% (19).

In terms of chemical effects, a range of photoprotective pigments such as melanins and carotenoids can be biosynthesized by fungi to quench ROS induced by UV radiation (20). Melanin derivatives are among the most common fungal pigments and are normally located in the cell wall and cytoplasm, acting as sunscreens (21). Studies in yeast species have also described a chemical response upon UV-B radiation through the increased biosynthesis of carotenoid compounds, which display a strong photoprotective activity (22, 23). For instance, strains of *Sporobolomyces salmonicolor* isolated from Antarctic environments accumulate sunscreen molecules as a response to UV-B exposure (24). During the stationary growth phase, high levels of carotenoids have been shown to enhance the chances of survival. Indeed, *Neurospora crassa*, which displays high levels of carotenoids, was more tolerant to UV radiation than *Neurospora discreta* or *Neurospora tetrasperma*, species containing low pigment content (25).

In Basidiomycetes, Boletales is a major order of ectomycorrhizal fungi, which form a range of fruiting body structures. Resupinate forms among the Boletales are brown-rotting saprotrophs preferably attacking coniferous woods (26). The major pigments associated with the order Boletales are atromentine-derived secondary metabolites, e.g., variegatic, xerocomic, isoxerocomic, and atromentic acids (27). While the ability of these compounds to absorb UV radiation has been established, their antioxidant and photoprotective properties have been poorly investigated. The study of pigments with strong UV quenching abilities is of great importance due to their potential application as radioprotective agents, which are widely used in medicine (28). To our knowledge, there is no report studying the chemical and morphological effects of UV-B radiation on *in vitro* cultures of any species in the order Boletales.

Serpula himantioides (Coniophoraceae), a resupinate member of Boletales, is widespread in Europe and the Americas, where it causes an intense brown rot on gymnosperms and more rarely on angiosperms (29, 30). This organism is commonly present in the south of Chile, where UV-B levels are increasing rapidly (31). Our work focused on the chemical and morphological changes of *in vitro* culture of *S. himantioides* upon controlled exposure to UV-B radiation. We quantified changes in growth rate and pigmentation, identifying xerocomic acid as the main pigment and characterizing its photoprotective properties.

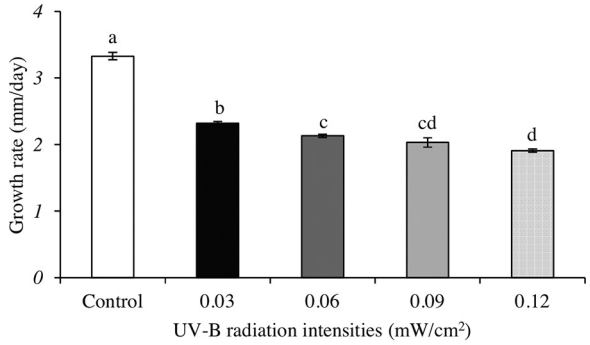

FIG 1 Effect of different intensities of UV-B radiation on growth rate (mm/day) of *in vitro* cultures of *S. himantioides*. Letters above the bars (a, b, c, and d) indicate statistical significance between experimental groups, where bars with different letters are significantly different ($P < 0.05$) and bars displaying the same letter show no significant differences between experimental groups ($P > 0.05$), as determined by one-way ANOVA followed by Tukey's multicomparison test.

RESULTS

UV-B radiation slows the hyphal growth rate of *S. himantioides* in *in vitro* culture. First, we confirmed our fungal sample to be *S. himantioides* by both morphological and molecular (DNA sequence) analyses (98 to 99% identity). Then, we began investigating the effect of UV-B exposure on the growth of this organism. The hyphal growth of *S. himantioides* was strongly affected by UV-B radiation, with increasing exposure corresponding to a decrease in growth. Under control conditions, the mycelium had covered the entire petri dish by the 25th day. In the presence of UV-B radiation, we observed a detrimental effect on *S. himantioides* over the course of the 25 days as well as with increasing dosage. The growth rate under different intensities of UV-B radiation was estimated (Fig. 1). Even at the lowest UV-B intensity (0.03 mW/cm^2), there was a significant decrease in the growth rate (2.32 mm/day) of *S. himantioides* in comparison to that of control experiments (3.33 mm/day). Intermediate intensities of 0.06 and 0.09 mW/cm^2 showed a progressive decline in the mycelial radial growth rate (2.13 and 2.03 mm/day, respectively). Finally, at the highest UV-B intensity (0.12 mW/cm^2), the growth rate of *S. himantioides* was 1.91 mm/day, which was significantly lower than that in nonradiated experiments. Additionally, at the highest UV-B intensity of 0.12 mW/cm^2, a substantial level of stress was induced in cultures of *S. himantioides* that resulted in a 50% reduction in the mycelial radial growth rate in solid culture media, in comparison to control experiments.

UV-B radiation alters pigment allocation but not thickness of the cell wall. Next, we considered the morphological response of *S. himantioides* upon exposure to UV-B. First, we used transmission electron microscopy to examine the hyphae from *in vitro* cultures of *S. himantioides* (Fig. 2). In the control experiment (Fig. 2a and b), pigmentation was homogeneously distributed within the hyphae. However, upon UV radiation, there was a reallocation of the pigment leading to the accumulation of pigment molecules near the cell wall, in comparison to control experiments (Fig. 2a and b). Exposure of *S. himantioides* to 0.03 and 0.06 mW/cm^2 of UV-B radiation led to a redistribution of the pigment toward the cell wall (Fig. 2c and d). At higher UV-B intensities (0.09 and 0.12 mW/cm^2), the reallocation of xerocomic acid near the cell wall was even more intense, as depicted in Fig. 2e and f. The more intense pigmentation of granules in radiated cultures compared with that of control experiments suggests increased production of xerocomic acid in samples exposed to UV-B. Although the increased pigmentation at 0.03 and 0.06 mW/cm^2 is not evident from the cross-section images in Fig. 2c and d, the culture medium of these experiments was clearly more darkly colored, indicating a higher content of the pigment than in control cultures.

We then investigated the effect of UV exposure on the cell wall. Figure 3 displays histograms showing the average cell wall thickness in the presence and absence of UV exposure. We found that UV-B radiation did not cause any significant change in the

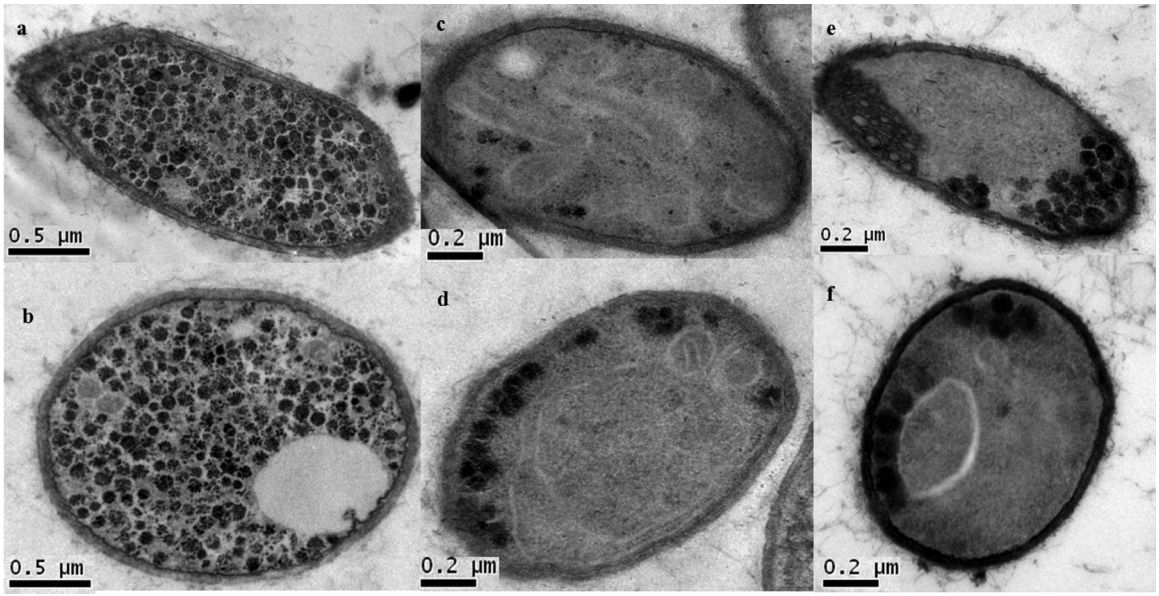

FIG 2 Cross-section transmission electron microscope images of hyphae from *in vitro* cultures of *S. himantioides* under different UV-B intensities. (a and b) Control (no radiation); (c) UV-B radiation at 0.03 mW/cm^2; (d) UV-B radiation at 0.06 mW/cm^2; (e) UV-B radiation at 0.09 mW/cm^2; (f) UV-B radiation at 0.12 mW/cm^2.

thickness of the cell wall. Average values of cell wall thickness from radiated *S. himantioides* were similar to those of the control experiments (Fig. 3).

UV-B radiation results in increased pigment composed largely of xerocomic acid. We observed that UV-B radiation had a strong effect on pigmentation of *S. himantioides*. After 25 days of UV-B treatment, the *in vitro* cultures of *S. himantioides* showed much higher pigment content than unexposed cultures (Fig. 4).

To understand the impact of changes in pigmentation, we aimed to determine the major secondary metabolites that are induced by UV-B radiation. We first analyzed *in*

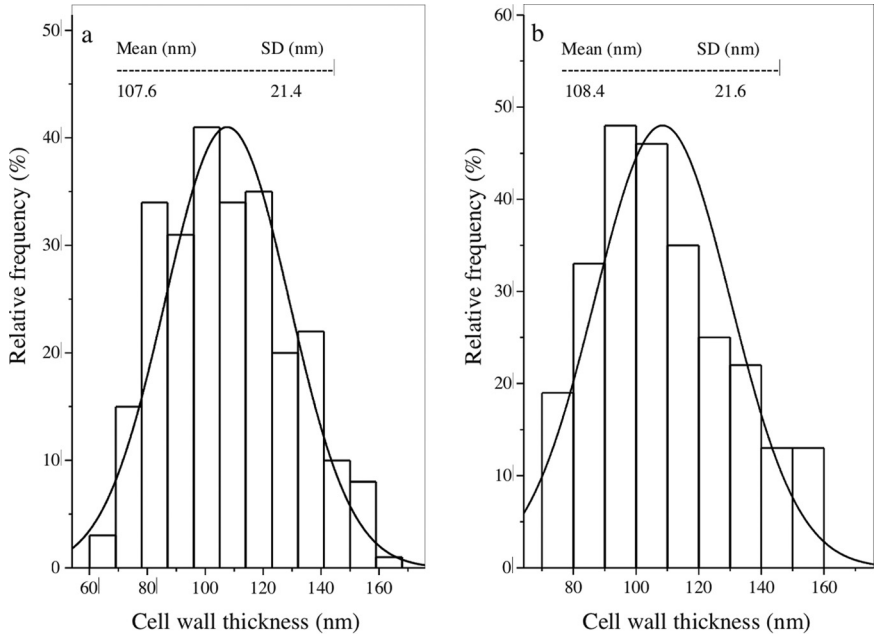

FIG 3 Histograms of cell wall thickness measured from cross sections of mycelium of *in vitro* cultures of the *S. himantioides* control (a) and with UV-B radiation at 0.12 mW/cm^2 (b). (Results were similar for all radiation intensities.)

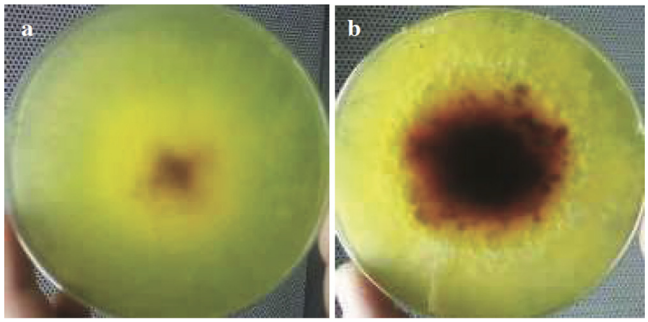

FIG 4 Pigmentation of *in vitro* cultures of *S. himantioides* after 25 days of growth with or without exposure to UV-B radiation. (a) Control; (b) UV-B radiation of 0.12 mW/cm^2.

vitro cultures of *S. himantioides* that were not stressed by UV-B radiation and found that xerocomic acid was the main pigment, with a concentration of 7 mg/liter after purification. High-performance liquid chromatography (HPLC) fractioning of *in vitro* cultures that were exposed to UV-B radiation (0.12 mW/cm^2) again revealed xerocomic acid as the main pigment, but in this case with a yield of 15 mg/liter (Fig. 5). We further checked that at a lower-intensity radiation (0.03 mW/cm^2), the production of xerocomic acid in *S. himantioides* also increased relative to that in control experiments (see Fig. S1 in the supplemental material). The chemical identification of xerocomic acid was confirmed by nuclear magnetic resonance (NMR) and mass spectrometry (MS).

***S. himantioides* extracts and xerocomic acid have antioxidant activities and photoprotective properties.** We investigated the antioxidant properties of total extracts as well as xerocomic acid, isolated from *in vitro* cultures of *S. himantioides*, using DPPH (2,2-diphenyl-1-picrylhydrazyl) and ABTS [2,2′-azino-bis(3-ethylbenzothiazoline-6-sulfonic acid) diammonium salt] assays. As displayed in Table 1, extracts from *S. himantioides* exposed to UV-B radiation showed impressive antioxidant activities in both assays, quantified as 3.15 mg/ml and 0.63 mg/ml, respectively.

Xerocomic acid was isolated from mycelium extracts of an *in vitro* culture of *S. himantioides*. We tested whether this pigment was the major contributor for the strong antioxidant activity displayed by extracts from irradiated *in vitro* cultures. Table 2 shows

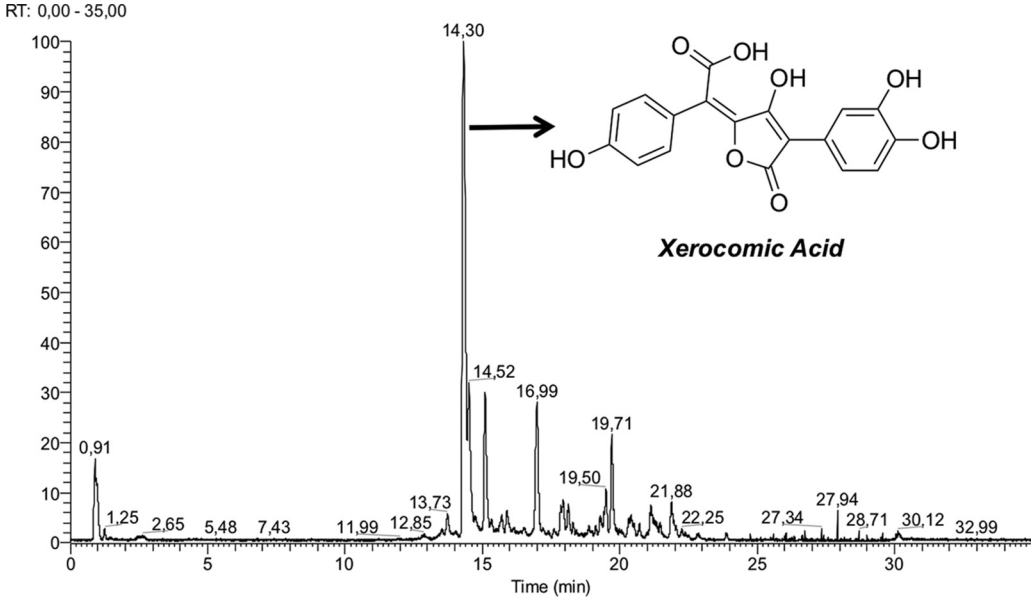

FIG 5 LC-MS chromatogram of total extract obtained from *in vitro* culture of *S. himantioides* exposed to UV-B radiation. Xerocomic acid is the major component (*Rt* [retention time] = 14.30).

TABLE 1 Antioxidant activity of total extracts from *in vitro* cultures of *S. himantioides*

Organism or reference standard	Treatment	Antioxidant activity (EC_{50}) (mg/ml)[a]	
		DPPH	ABTS
S. himantioides	Control	8.87 ± 0.5	2.80 ± 0.4
	UV	3.15 ± 0.3	0.63 ± 0.4
Trolox		0.02 ± 0.4	0.03 ± 0.4

[a]EC_{50}, concentration of extract at which 50% of the employed radical was quenched. Values are the means of results for triplicate experiments ± SD.

the antioxidant properties of xerocomic acid isolated from UV-B-exposed cultures, as measured by the DPPH, ABTS, and oxygen radical absorbance capacity (ORAC) assays. The ORAC assay was included in order to give a broader antioxidant characterization to xerocomic acid. These experiments showed that xerocomic acid has high levels of antioxidant activity: DPPH, 0.34 mg/ml; ABTS, 0.036 mg/ml; and ORAC, 22.58 μmol Trolox equivalents (TE)/ml. These values are comparable to well-known antioxidant standards (32–34). A potential concern was that the presence of laccases could interfere with the ABTS assay. In order to verify that laccases were not present in our system, we tested for their presence in *S. himantioides*. We found no laccase activity (Fig. S2).

We hypothesized that the increased xerocomic acid may also have photoprotective properties. To test this, we employed the MTT [3-(4,5-dimethyl-2-thiazolyl)-2,5-diphenyl-2H-tetrazolium bromide] assay to evaluate the protective effect of xerocomic acid on cytotoxicity in the HEK293 cell line and compared it with β-carotene, which is known to have a photoprotective effect (Fig. 6). Exposure of HEK293 cell lines to UV-B radiation without xerocomic acid resulted in 76% (Fig. 6a, white bar). Interestingly, xerocomic acid displayed strong photoprotective properties at all the concentrations tested (Fig. 6a, yellow bars). Remarkably, at 0.1 mM, the xerocomic acid pigment protected HEK293 cell lines from harmful UV-B radiation, leading to a viability of 99% ± 5.0%. Xerocomic acid showed even stronger photoprotective properties than β-carotene at the same concentrations.

Although xerocomic acid leads to increased viability in the presence of UV-B, it may have detrimental effects when UV-B is not present. In order to evaluate the potential toxic properties of xerocomic acid, HEK293 cells were incubated for 5 h in the presence of xerocomic acid at different concentrations (0.05 to 0.4 mM) under UV-B-free conditions (Fig. 6b). Results of the MTT assay indicated that xerocomic acid does display mild cytotoxic effects on nonirradiated HEK293 cells, in comparison to a positive control for toxicity experiments (FCCP [carbonyl cyanide-4-trifluoromethoxyphenylhydrazone]). At 0.05 mM and 0.1 mM concentrations of xerocomic acid, the viability was reduced marginally to 97% ± 3.9% and 92% ± 4.2%, respectively. Even at higher concentrations, the pigment toxicity was still relatively modest, with 82% ± 4.1% (0.2 mM) and 75% ± 2.1% (0.4 mM) of viability.

DISCUSSION

Our study shows the morphological and chemical responses of *S. himantioides* to controlled intensities of UV-B radiation under *in vitro* culture conditions. This adds a new order of fungi to the growing set of observations about how different fungi

TABLE 2 Antioxidant activity of xerocomic acid

Pigment or reference standard	Treatment	Antioxidant activity[a]		
		DPPH EC_{50} (mg/ml)	ABTS EC_{50} (mg/ml)	ORAC (μmol TE/ml)
Xerocomic acid	UV	0.34 ± 0.1	0.04 ± 0.1	22.58 ± 0.63
Trolox		0.02 ± 0.2	0.03 ± 0.4	

[a]EC_{50}, concentration of extract at which 50% of the employed radical was quenched; TE, Trolox equivalents. Values are the means of results for triplicate experiments ± SD.

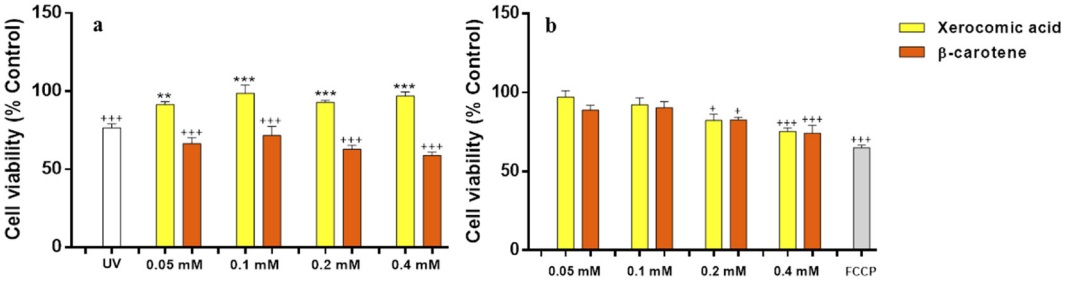

FIG 6 Effect of xerocomic acid on HEK293 cell viability. (a) HEK293 cells exposed to UV-B (0.12 mW/cm^2) in the presence of increasing concentrations of xerocomic acid or β-carotene as a positive control. The bar labeled UV represents cells without pigment. (b) HEK293 cells not exposed to UV-B radiation (control plate) but with the same increasing concentrations of xerocomic acid or β-carotene. FCCP (10 μM) was used as a positive control for toxicity. The results are expressed as a percentage of the result for untreated, unexposed cells, with triplicate experiments for each treatment. The following symbols indicate results that were considered statistically significant: $^+$, $P < 0.05$; $^{++}$, $P < 0.01$; and $^{+++}$, $P < 0.001$ (versus the control); *, $P < 0.05$; **, $P < 0.01$; and ***, $P < 0.001$ (versus UV-B treatment).

respond to UV radiation. First, we found that the growth rate was substantially lower upon UV-B exposure. We observed a decrease in the hyphal growth of *S. himantioides* at all the intensities tested, with a strong effect already observed with the smallest UV-B radiation intensity (0.03 mW/cm^2). Higher UV-B intensities (0.06, 0.09, and 0.12 mW/cm^2) further depressed the growth, but to a lesser degree. Decreased growth following UV-B radiation is thought to be a survival strategy employed by some fungi (35) as a way to channel metabolic efforts toward the biosynthesis of molecules with photoprotective abilities. For example, negative effects of radiation exposure on growth parameters have been reported for some entomopathogenic fungi such as *Beauveria bassiana* (36). Several filamentous fungi have also been shown to have slower growth following UV radiation (37, 38), including five species from Antarctic environments (39).

Besides the effect on growth rate, we did not observe significant morphological changes in cell wall thickness of *S. himantioides* upon UV-B exposure. We did, however, observe pigmentation changes associated with the UV-B exposure. Electron microscopy analysis revealed an intense increase in pigment content as well as reallocation of pigment near the cell wall in response to UV-B radiation. However, cell wall thickness itself was not affected by UV-B treatment. Other morphological responses may occur, such as changes in cell size. Indeed, the results of the electron microscopy experiments (Fig. 2) are consistent with a decrease in cell size in UV-B-exposed *S. himantioides*. However, further experiments and larger numbers of assays are needed to address this. In other fungi, accumulation of carotenoid-derived pigments in hyphae, spores, cytoplasm, and cell membranes (40) has been reported. In lichens exposed to UV radiation, molecules displaying sun-protective properties have been isolated, including lobaric acid, pannarin, atranorin, gyrophoric acid, epiforelic acids, secalonic acids, mycosporine, melanin, and carotenoid-derived pigments (9). Analysis of extracts by NMR and mass spectrometry revealed that xerocomic acid was the main pigment present both before and after UV exposure, with levels of this pigment substantially higher in cultures irradiated with UV-B. It is known that mushrooms of the order Boletales biosynthesize terphenylquinones, pulvinic acids, and shikimate-derived pigments (27, 41). Variegatic and xerocomic acids are exclusively present in the order Boletales (42), but the effect of UV radiation on changes in pigmentation was previously unknown.

Traditionally, microorganisms counteract the harmful effect of UV radiation by activating metabolic pathways that produce molecules with antioxidant and photoprotective properties (41). In fungi, compounds with photoprotective abilities play a crucial role in neutralizing ROS (43). Previous reports have shown that pulvinic acid derivatives display antioxidant properties. For example, a previous study showed that norbadione A, which has a chemical structure containing two subunits similar to xerocomic acid, exhibits antioxidant bioactivities (28). Thus, we proceeded to investigate the antioxidant and photoprotective properties of total extracts and xero-

comic acid isolated from cultures of *S. himantioides* under *in vitro* conditions. Consistently, the antioxidant properties of this extract and the pigment were quantified to be high by means of all three assays used. The 50% effective concentration (EC_{50}) of methanolic extract from mycelia exposed to UV-B radiation rendered values of 3.15 mg/ml and 0.63 mg/ml for DPPH and ABTS, respectively. In contrast, extracts from nonirradiated cultures displayed low antioxidant activities, 8.87 ± 0.5 mg/ml (DPPH) and 2.80 ± 0.4 mg/ml (ABTS). The antioxidant activity cannot be due to a confounding effect from the presence of laccase, since we found that *S. himantioides* was unable to oxidize ABTS in a screening assay for laccase production, consistent with the lack of laccase-related metabolic pathways in other related brown-rotting fungi (44). Thus, the difference in antioxidant strength can be attributed to the increased amounts of xerocomic acid present in the cultures of *S. himantioides* that were exposed to UV radiation. The antioxidant activities displayed by *S. himantioides* are even higher than those found in other *in vitro* studies of fungi (*Cordyceps*) exposed to UV radiation (45, 46). Antioxidant properties of other Boletales fungi have been investigated in previous reports, but not under *in vitro* conditions (47–51). Melanin and carotenoid derivatives are a family of compounds with strong antioxidant activity (52). However, xerocomic acid displayed better antioxidant properties than fungal melanin compounds (53), demonstrating the notable potential of this pigment as a new antioxidant agent.

In addition, the photoprotective ability of xerocomic acid was evaluated on HEK293 cells. We found that xerocomic acid was able to protect this cell line from UV radiation more efficiently than β-carotene, which was used as a positive control. Carotene derivatives act as light filters and thus prevent oxidative stress, but we also observed that in the presence of UV radiation, this pigment decreased cellular viability at all concentrations tested. The photoprotective properties of β-carotene and other antioxidants (lycopene, vitamins E and C, and carnosic acid) are known for their ability to protect against photoaging in primary cultures of human dermal fibroblasts irradiated with UV (54). In our investigation, xerocomic acid was better tolerated by HEK293 cells and showed only modest cytotoxicity even at high concentrations (0.2 and 0.4 mM). Remarkably, at all the concentrations tested, xerocomic acid proved to protect HEK293 cells from UV radiation without causing cytotoxicity. These features indicate exciting potential for this pigment as a new antioxidant and photoprotective agent. It has been reported that vulpinic acid, an analogue to xerocomic acid, did not show cytotoxic effects on nonirradiated HaCaT cells (MTT cell viability assay [55]). Interestingly, vulpinic acid prevented almost all the toxic effects of UV-B radiation and was found to be more protective and promising than α-tocopherol, which was used as a positive control.

In summary, we report the morphological and chemical adaptive responses of *S. himantioides*, under *in vitro* conditions, in the presence of controlled intensities of UV-B radiation. A decrease in growth rate, but no change in cell wall thickness, was observed following UV-B exposure. Moreover, xerocomic acid was shown to have substantial antioxidant and photoprotective abilities. Thus, our results suggest that upon UV-B exposure, *S. himantioides* decreases its hyphal growth rate and uses this energy instead to increase the biosynthesis of xerocomic acid, which is allocated near the cell wall. This metabolic switch likely allows xerocomic acid to efficiently defend *S. himantioides* from UV radiation through its antioxidant and photoprotective properties. These findings suggest that xerocomic acid is a promising UV protecting agent and should therefore be investigated in depth in the near future.

MATERIALS AND METHODS

Chemicals. 2,2′-Azino-bis(3-ethylbenzothiazoline-6-sulfonic acid) diammonium salt (ABTS), 6-hydroxy-2,5,7,8-tetramethylchromane-2-carboxylic acid (Trolox), 2,2-diphenyl-1-picrylhydrazyl (DPPH), 2,2′-azobis(2-amidinopropane)dihydrochloride (AAPH), fluorescein, β-carotene, and 3-(4,5-dimethylthiazol-2-yl)-2,5-diphenyltetrazolium bromide (MTT) were purchased from Sigma-Aldrich. Dulbecco's modified Eagle's medium (DMEM), Dulbecco's phosphate-buffered saline (DPBS), fetal bovine serum (FBS), and penicillin-streptomycin were purchased from Thermo Fisher Scientific. Acetonitrile and water were HPLC grade. All chemicals were analytical grade. A high-quality reference of xerocomic acid was obtained from the in-house compound library at Leibniz Institute of Plant Biochemistry (donated by W. Steglich, Ludwig

Maximilian University of Munich). Reagents were used without further purification. Milli-Q-grade water was used during the entire process.

Sample collection. *S. himantioides,* from the order Boletales, was collected from decomposing wood in a native Chilean forest in the Bíobío region (Zona Central) of Chile (36°50′15″S, 73°01′30″W) in autumn 2014. Species identification was based on both macroscopic and microscopic features as well as DNA sequence (described below), by comparison with references. The reference material has been deposited in the fungal collection at the Universidad de Concepcion (accession number CONC-F 1792).

Macroscopic and microscopic identification of *S. himantioides*. The collected material was analyzed macroscopically in a fresh state both *in situ* and *in vitro*. Macroscopic features, including size, spore color, and type of fructification, were all positively identified as *S. himantioides*. Microscopic observations of fresh material were conducted using a Leitz Dialux microscope (×1,000 magnification, immersion objective; Leitz, Wetzlar, Germany) equipped with a camera (56). Microscopic features, such as septate hyphae, presence of fibulae, and hyphal size, were also congruous with *S. himantioides*.

Isolation and cultures of fungi. Culture preparation was performed as previously described (30). Mycelial cultures of *S. himantioides* were derived from the spore print of a fruiting body. The strain was kept on a petri dish (90-mm diameter) containing potato dextrose agar (PDA) medium composed of 4 g/liter potato extract, 20 g/liter dextrose, and 15 g/liter agar, with the pH adjusted to 5.6. The mycelium used for inoculation was taken from the surface of the agar medium, and the piece of mycelium from the agar (4 by 4 mm) was inoculated onto the liquid medium. The liquid culture fermentation was maintained in 2-liter flasks containing potato dextrose broth (PDB) medium without shaking at 24°C for 25 days.

Molecular identification of *S. himantioides*. DNA was extracted from pure mycelium cultures using potato dextrose agar (PDA), according to CTAB methodology (57). The region corresponding to the internal transcribed spacer (ITS) was amplified via PCR using the primers ITS1F (5′-CTTGGTCATTTAGAG GAAGTAA-3′) and ITS4 (5′-TCCTCCGCTTATTGATATGC-3′) (58). PCR conditions were as follows: 94°C for 4 min, followed by 30 cycles at 94°C for 40 s, 60°C for 40 s, and 72°C for 1 min, and then a final elongation at 72°C for 10 min. The PCR products were sequenced by Macrogen (Korea), and the sequence was deposited in GenBank (accession number MK694772). A BLASTn search of the sequence against the NCBI database (59) results shows 98% to 99% identity with other *S. himantioides* ITS sequences.

UV-B radiation of *in vitro* cultures. A petri dish containing culture medium was subjected to UV-B radiation. The intensity was determined using a radiometer equipped with an external sensor. The range was 290 to 390 mm (PCE-UV34), and the measurements were given in mW/cm² using a fluorescent UV-B broadband TL lamp (Philips TL 20 W/12 RS SLV) (16). The UV-B intensities were 0.03, 0.06, 0.09, and 0.12 mW/cm² for 3 h over 25 days for evaluation of hyphal growth. Cultures that were not exposed to UV-B radiation were considered control experiments (60).

In vitro cultures of *S. himantioides* were subjected to UV-B radiation once the hyphae of such cultures reached 3 mm in length (39). Petri dishes were covered with a transparent film to avoid cross-contamination and stored in an incubator at 25°C between radiation experiments.

The effect of radiation on secondary metabolites of *S. himantioides* was studied using high-intensity UV-B energy (0.12 mW/cm²), which is similar to the UV-B radiation levels in the south of Chile (61, 62). *In vitro* cultures were performed using 2-liter flasks that were kept at 25°C for the entire experiment. In order to standardize the radiation surface, the culture medium was transferred to rectangular glass containers in which the UV-B radiation was applied with a lamp placed at a distance of 35 cm from the cultures. The radiation method was as before: 3 h per day, over 15 days. Mycelial cultures that were not exposed to UV-B radiation were grown in parallel as control experiments.

Evaluation of hyphal growth and inhibition rate of *S. himantioides*. The effect of UV-B radiation on the radial mycelial growth was determined by measuring the spread of *S. himantioides* along the petri dish in four directions using a caliper and a magnifying glass (63). These measurements were done in triplicate, every other day, using a digital caliper until mycelia covered the entire petri plate (25 days). Using the obtained measurement data (in mm), the hyphal growth rate and inhibition percentage were calculated for all four UV-B intensities and a linear regression was fit to calculate the growth rate (mm/day) for the four different UV-B intensities (64). The inhibition percentage was calculated for days 5, 15, and 25, as well as for control experiments. The equation used has been previously described (65):

$$\%\,\text{Inhibition} = \frac{\text{growth of control} - \text{growth of sample}}{\text{growth of control}} \times 100$$

Transmission electron microscopy. Mycelium samples were obtained from solid culture medium of *S. himantioides* after the 25-day radiation treatment. Morphological changes were studied by fixing mycelium samples with paraformaldehyde (2%, vol/vol) containing 2.5% glutaraldehyde–0.1 M phosphate buffer (pH 7.2) for 4 h at 23°C. After the fixation stage, samples were subjected to dehydration and resin inclusion (66). Fifty transversal sections were measured in four directions to determine the width (mm) of the hyphal cell wall for each UV-B radiation treatment. Data were plotted as histograms using Origin Pro 6.1. A JEOL JSM 1200EX-II (1994) transmission electron microscope was used.

Acquisition and purification/fractionation of total extracts. Total extracts were obtained from each of the *in vitro* cultures of *S. himantioides* subject to different intensities of UV-B radiation. Cultures were filtered, and yields were calculated (mg/liter). Broth cultures were extracted with ethyl acetate (three times, 250 ml each time), and the extract was concentrated until dry using a rotatory evaporator (Heildolph Unimaz 2010).

The crude extract of *S. himantioides* containing pigments was subjected to flash chromatography using Sephadex LH-20 with acetone and methanol in a 4-to-1 ratio as the eluent. All fractions containing pigments were collected and further purified using HPLC.

NMR analysis. One-dimensional (^{1}H, ^{13}C) nuclear magnetic resonance (NMR) spectra were obtained from an Agilent VNMRS 600 system at 25°C. The pure compounds were dissolved in acetone-d6 (99.96% deuterated), and spectra were recorded at 599.83 MHz (^{1}H) and 150.84 MHz (^{13}C), respectively. The structure of xerocomic acid was elucidated on the basis of spectroscopic analysis and chemical evidence (67).

Preparative HPLC for isolation of pigments. Fractions containing pigment (68 mg) were further purified using preparative HPLC. The HPLC purification was performed on a Varian ProStar RP HPLC system with a LiChroCART 250-10 column and LiChrospher 100 RP-18 (10 μm) carrier (Merck, Darmstadt, Germany), using H_2O (A) and CH_3CN (B) as eluents (linear gradient, 0 to 22 min, 2% to 100% B, flow rate of 4 ml min^{-1}), yielding xerocomic acid.

HPLC-MS analysis. Each sample (2 μl) was loaded on a Hypersil GOLD column (C_{18}, inside diameter of 2.1 mm, length of 50 mm, particle size of 1.9 μm; Thermo Fisher Scientific) using a Dionex 3000 ultra-HPLC (UHPLC), equipped with a WPS-3000 TRS autosampler, an LPG-3400RS binary pump, a TCC-3000RS column oven, and a DAD-3000 photodiode array detector (Thermo Fisher Scientific, Bremen, Germany). The eluents A and B were water and acetonitrile, respectively, both containing 0.1% (vol/vol) formic acid. After a 4-min isocratic step (5% eluent B), analytes were eluted at a flow rate of 150 μl/min at 30°C in a linear gradient to 100% eluent B in 15 min. The column effluents were introduced on-line in an Orbitrap Elite mass spectrometer via a HESI source (Thermo Fisher Scientific, Bremen, Germany). The instrument was operated in the negative ion mode and controlled by Xcalibur software (Thermo Fisher Scientific, Bremen, Germany).

Antioxidant assays. Three different assays, a free-radical scavenging DPPH assay, the ABTS radical cation scavenging assay, and the ORAC assay, were used to evaluate the antioxidant potential of fungal extracts. Each experiment was done in triplicate, and mean values were taken.

DPPH assay. The DPPH free-radical method is an antioxidant assay based on an electron transfer process, which gives a strong purple color in methanol (47). The free radical is stable at room temperature but can be reduced in the presence of an external antioxidant molecule, rendering a colorless methanol solution. Thus, the DPPH assay provides a rapid protocol to evaluate antioxidants by spectrophotometry (47). The antioxidant activities of the extracts and xerocomic acid were measured on the basis of the scavenging activity of the DPPH free radical. One hundred eighty microliters of 100 μM DPPH solution in methanol was mixed with 20 μl of methanolic extracts of various concentrations (0.25, 0.5, 1.0, 2.0, 4.0, and 8.0 mg/ml) and 20 μl xerocomic acid (10, 20, 40, 60, 800, and 100 μg/ml), respectively. Trolox was used as a standard (68). Trolox is a water-soluble antioxidant derived from vitamin E that is commonly used as a standard antioxidant for antioxidant assays (69). The antioxidant capacities of extracts and xerocomic acid, given by the percent inhibition of the DPPH free radical, were compared with the values rendered by Trolox. The percent inhibition by extracts and xerocomic acid was calculated using the following formula:

$$\text{DPPH scavenging activity (\%)} = \frac{(A_{\text{control}} - A_{\text{sample}})}{A_{\text{control}}} \times 100$$

where A_{control} is the absorbance of the solvent plus DPPH at 515 nm and A_{sample} is the absorbance of the sample plus DPPH at 515 nm.

The EC_{50} (mg/ml) was determined as the effective concentration in which the DPPH radicals are 50% quenched. Absorbance measurements were taken using an ELX800 microplate reader (BioTek Instruments, Inc., Winooski, VT) at 515 nm.

ABTS assay. The ABTS assay is based on the inhibition of the absorbance of the radical cation of ABTS, which has a characteristic long-wavelength absorption spectrum showing a maximum at 734 nm (70). Stock solutions of 3.75 mM ABTS and 1.23 mM potassium persulfate ($K_2S_2O_8$; Merck KGaA, Darmstadt, Germany) were mixed and stored in the dark at 30°C overnight. The resulting solution was then diluted in methanol until 0.6 $\pm$ 0.05 of absorbance (734 nm) was reached. Twenty microliters of methanolic extracts of various concentrations (0.25, 0.5, 1.0, 2.0, 4.0, and 8.0 mg/ml) and 20 μl of xerocomic acid (10, 20, 40, 60, 800, and 100 μg/ml) were mixed with 180 μl of ABTS solution. Trolox was used as the standard (71). The percent inhibition was calculated using the following equation:

$$\text{ABTS scavenging activity (\%)} = \frac{A_{\text{control}} - A_{\text{sample}}}{A_{\text{control}}} \times 100$$

where A_{control} is the absorbance of the solvent plus ABTS at 734 nm and A_{sample} is the absorbance of the sample plus ABTS at 734 nm.

The EC_{50} (mg/ml) was determined as the effective concentration in which the ABTS radicals are 50% quenched. Absorbance measurements were taken using an ELX800 microplate reader (BioTek Instruments, Inc., Winooski, VT) at 734 nm.

ORAC assay. The oxygen radical absorbance capacity (ORAC) assay was performed according to previously described protocols (72). In brief, this is an assay that measures antioxidant activity and is based on a hydrogen atom transfer (HAT) mechanism (73). This assay entails a competition reaction between antioxidants and a fluorescence probe for a radical, usually a peroxy radical generated from AAPH. Trolox is used, in a separate experiment, as an antioxidant standard since it quenches the peroxy radical formed from AAPH, protecting the fluorescein from radical decay. A calibration curve is generated using Trolox, and samples are compared to these data. Specifically, 1 mg/ml of xerocomic acid was

dissolved in dimethyl sulfoxide (DMSO). Phosphate buffer (0.075 M) was used as a blank. ORAC values of xerocomic acid were calculated using a calibration curve prepared with Trolox (5 to 30 μM). One hundred fifty microliters of fluorescein working solution (11×10^{-2} μM) was mixed with 25 μl of the sample. The resulting solution was incubated at 37°C for 30 min. Then, 25 μl of AAPH (600 mM) was added to each well. The plate was then immediately transferred to the plate reader, and the fluorescence was measured every minute for 35 min. The final ORAC values were calculated using the regression equation between the Trolox concentration and the area under the curve (AUC), with ORAC values expressed as Trolox equivalents (TE) per milliliter of sample (μmol · TE/ml).

Toxicity and photoprotective properties on HEK293 cells. The effect of xerocomic acid on the viability of HEK293 cells and photoprotection after UV-B irradiation was assessed by an MTT colorimetric assay.

Xerocomic acid for biological assays (sample preparation). Stock solutions of dry xerocomic acid (100 mM) were prepared in Dulbecco's phosphate-buffered saline (DPBS) and stored at −4°C until analysis. Dry xerocomic acid (100 mM) was dissolved in DPBS and used as a stock solution. For the following assays, extracts were subjected to two serial dilutions in DPBS (1 and 10 mM), reaching the following concentrations: 0.05, 0.1, 0.2, and 0.4 mM (55).

Cell culture. Human embryonic kidney cells (HEK293; American Type Culture Collection [ATCC], Manassas, VA, USA) were employed as model cells since they are epithelium adherent, like normal human keratinocytes, but much easier to handle. HEK293 cells were grown in DMEM supplemented with fetal bovine serum (5%), horse serum (5%), and penicillin and streptomycin (1%) and kept in a thermoregulated incubator at 37°C with 5% CO_2. To evaluate viability, cells were plated at a concentration of 30,000 cells/well and used after reaching 80% confluence.

Photoprotective activity. In order to investigate the cytotoxic effects of UV-B irradiation on HEK293 cells, and the photoprotective properties of xerocomic acid, cell viability was evaluated using an MTT assay, which reflects cellular metabolic activity. A modified protocol from previous work was used (55). Two microplates per assay were prepared to evaluate the photoprotective activity of xerocomic acid. At 80% confluence, the medium was replaced by normal external solution (NES). The HEK293 cells were treated with 0.05, 0.1, 0.2, and 0.4 mM xerocomic acid in DPBS and incubated for 30 min. One of the microplates was irradiated with 0.12 mW/cm^2 using a UV-B broadband TL fluorescent lamp (Philips TL 20 W/12 RS SLV) for 1 min, and then the lamp was turned off for 5 min; this was repeated three times. The lamp was positioned 35 cm from the microplate, and the absorbance was recorded after 4 h. The second microplate containing the xerocomic acid was incubated in the dark during the entire experiment. It was not exposed to UV-B and was considered a negative control. In one microplate, NES was replaced by DMEM supplemented with 10% fetal bovine serum β-carotene as a positive control. Cellular viability was determined by the MTT assay.

Cell viability assay. Cell viability was assessed on the HEK293 cell line (74). The xerocomic acid was tested for *in vitro* cytotoxicity, using HEK293 cells, by an MTT assay as previously described (75). Briefly, cultures were incubated with MTT (5 mg/ml) for 30 min. The precipitated MTT was then dissolved using isopropanol for 15 min. The absorbance was measured in a NOVOstar microplate reader (BGM, Germany) at 570 nm for the different experimental conditions, and the viability percentage was calculated as follows:

$$\%\,\text{Viability of cells} = \frac{(\text{absorbance of sample} - \text{absorbance of blank})}{(\text{absorbance of control} - \text{absorbance of blank})} \times 100$$

Statistical analysis. The effect of UV-B treatments on growth rates (mm/day) was evaluated by one-way analysis of variance (ANOVA). Tukey's honestly significant difference test was employed. The fit to a normal distribution was confirmed via the Shapiro-Wilk and Levene tests. All analyses were performed using the software GraphPad Prism (GraphPad, CA, USA).

Accession number(s). The DNA sequence for *S. himantioides* was deposited in GenBank under accession number MK694772.

SUPPLEMENTAL MATERIAL

Supplemental material for this article may be found at https://doi.org/10.1128/AEM.00870-19.

SUPPLEMENTAL FILE 1, PDF file, 1.3 MB.

ACKNOWLEDGMENT

This research was funded by postdoctoral FONDECYT project no. 3180635, FONDECYT regular project no. 1151028, and FONDECYT regular project no. 1190652.

We are grateful to Ricardo Oliva in the Spectroscopy and Microscopy Center (CESMI) at the University of Concepcion for his contribution to electronic transmission microscopy and Andrej Frolov from the Leibniz Institute of Plant Biochemistry (IPB), Halle, Germany, for his help in LC-MS analysis. We also thank Ellen Leffler for critical reading of the manuscript and Katia Saez Carrillo from the Statistics Department at the University of Concepcion for her useful suggestions in statistical analysis.

We declare no conflicts of interest.

REFERENCES

1. Bornman JF, Barnes PW, Robinson SA, Ballaré CL, Flint SD, Caldwell MM. 2015. Solar ultraviolet radiation and ozone depletion driven climate change: effects on terrestrial ecosystems. Photochem Photobiol Sci 14:88–107. https://doi.org/10.1039/c4pp90034k.
2. de Jager TL, Cockrell AE, Du Plessis SS. 2017. Ultraviolet light induced generation of reactive oxygen species. Adv Exp Med Biol 996:15–23. https://doi.org/10.1007/978-3-319-56017-5_2.
3. Yokawa K, Kagenishi T, Baluška F. 2016. UV-B induced generation of reactive oxygen species promotes formation of BFA-induced compartments in cells of Arabidopsis root apices. Front Plant Sci 6:1–10. https://doi.org/10.3389/fpls.2015.01162.
4. Carletti G, Nervo G, Cattivelli L. 2014. Flavonoids and melanins: a common strategy across two kingdoms. Int J Biol Sci 10:1159–1170. https://doi.org/10.7150/ijbs.9672.
5. Rastogi RP, Richa, Kumar A, Tyagi MB, Sinha RP. 2010. Molecular mechanisms of ultraviolet radiation-induced DNA damage and repair. J Nucleic Acids 2010:592980. https://doi.org/10.4061/2010/592980.
6. Gessler NN, Egorova AS, Belozerskaya TA. 2014. Melanin pigments of fungi under extreme environmental conditions (review). Appl Biochem Microbiol 50:105–113. https://doi.org/10.1134/S0003683814020094.
7. Shu LX, Hui FZ, Min HP. 2014. Effects of solar radiation on photosynthesis and pigmentation in the red alga *Pyropia yezoensis* Ueda (Bangiales, Rhodophyta). Indian J Geomarine Sci 43:473–480.
8. Llabrés M, Agustí S, Fernández M, Canepa A, Maurin F, Vidal F, Duarte CM. 2013. Impact of elevated UVB radiation on marine biota: a meta-analysis. Glob Ecol Biogeogr 22:131–144. https://doi.org/10.1111/j.1466-8238.2012.00784.x.
9. Nguyen KH, Krugler MC, Gouault N, Tomasi S. 2013. UV-protectant metabolites from lichens and their symbiotic partners. Nat Prod Rep 30:1490–1508. https://doi.org/10.1039/c3np70064j.
10. Singh J, Singh RP, Dubey AK. 2012. Effects of ultraviolet-B (UV-B) radiation on two cryptogamic plants pigments growing at high altitude of central Himalayan region, India. Afr J Environ Sci Tech 6:9–16.
11. Solhaug KA, Gauslaa Y, Nybakken L, Bilger W. 2003. UV-induction of sun-screening pigments in lichens. New Phytol 158:91–100. https://doi.org/10.1046/j.1469-8137.2003.00708.x.
12. Choi J, Kim SH. 2017. A genome tree of life for the Fungi kingdom. Proc Natl Acad Sci U S A 114:9391–9396. https://doi.org/10.1073/pnas.1711939114.
13. Knox BP, Keller NP. 2015. Key players in the regulations of fungal secondary metabolism, p 13–28. *In* Zeilinger S, Martín JF, García-Estrada C (ed), Biosynthesis and molecular genetics of fungal secondary metabolite, 1st ed, vol 2. Springer, New York, NY.
14. Gmoser R, Ferreira JA, Lennartsson PR, Taherzadeh MJ. 2017. Filamentous ascomycetes fungi as a source of natural pigments. Fungal Biol Biotechnol 4:4. https://doi.org/10.1186/s40694-017-0033-2.
15. Allam NG, Abd El- Zaher EHF. 2012. Protective role of *Aspergillus fumigatus* melanin against ultraviolet (UV) irradiation and *Bjerkandera adusta* melanin as a candidate vaccine against systemic candidiasis. Afr J Biotechnol 11:6566–6577.
16. Libkind D, Moline M, van Broock M. 2011. Production of the UVB-absorbing compound mycosporine-glutaminol-glucoside by *Xanthophyllomyces dendrorhous* (*Phaffia rhodozyma*). FEMS Yeast Res 11:52–59. https://doi.org/10.1111/j.1567-1364.2010.00688.x.
17. Fourtouni A, Manetas Y, Christias C. 1998. Effects of UV-B radiation on growth, pigmentation, and spore production in the phytopathogenic fungus *Alternaria solani*. Can J Bot 76:2093–2099. https://doi.org/10.1139/b98-170.
18. García-Cela E, Marin S, Sanchis V, Crespo-Sempere A, Ramos AJ. 2015. Effect of ultraviolet radiation A and B on growth and mycotoxin production by *Aspergillus carbonarius* and *Aspergillus parasiticus* in grape and pistachio media. Fungal Biol 119:67–78. https://doi.org/10.1016/j.funbio.2014.11.004.
19. Yamaga I, Kuniga T, Aoki S, Kato M, Kobayashi Y. 2016. Effect of ultraviolet-B irradiation on disease development caused by *Penicillium italicum* in Satsuma mandarin fruit. Hortic J 85:86–91. https://doi.org/10.2503/hortj.MI-074.
20. Pombeiro-Sponchiado SR, Sousa GS, Andrade J, Lisboa HF, Gonçalves R. 2017. Production of melanin pigment by fungi and its biotechnological applications, p 47–75. *In* Blumenberg M (ed), Melanin, 1st ed. IntechOpen, New York, NY.
21. Olaizola C, Abramowski ZA, Ayala EM. 2013. Photoprotective effect of fungal melanins against UVB in human skin cells. Micol Aplicada Int 25:3–12.
22. Libkind D, Pérez P, Sommaruga R, Diéguez M, Ferraro M, Brizzio S, Zagarese H, van Broock M. 2004. Constitutive and UV-inducible synthesis of photoprotective compounds (carotenoids and mycosporines) by freshwater yeasts. Photochem Photobiol Sci 3:281–286. https://doi.org/10.1039/B310608J.
23. Villarreal P, Carrasco M, Barahona S, Alcaíno J, Cifuentes V, Baeza M. 2016. Tolerance to ultraviolet radiation of psychrotolerant yeasts and analysis of their carotenoid, mycosporine, and ergosterol content. Curr Microbiol 72:94–101. https://doi.org/10.1007/s00284-015-0928-1.
24. Dimitrova S, Pavlova K, Lukanov L, Korotkova E, Petrova E, Zagorchev P, Kuncheva M. 2013. Production of metabolites with antioxidant and emulsifying properties by Antarctic strain *Sporobolomyces salmonicolor* AL_1. Appl Biochem Biotechnol 169:301–311. https://doi.org/10.1007/s12010-012-9983-2.
25. Luque EM, Gutiérrez G, Navarro-Sampedro L, Olmedo M, Rodríguez-Romero J, Ruger-Herreros C, Tagua VG, Corrochano LM. 2012. A relationship between carotenoid accumulation and the distribution of species of the fungus Neurospora in Spain. PLoS One 7:e33658. https://doi.org/10.1371/journal.pone.0033658.
26. Binder M, Hibbett DS. 2006. Molecular systematics and biological diversification of Boletales. Mycologia 98:971–981. https://doi.org/10.1080/15572536.2006.11832626.
27. Velíšek J, Cejpek K. 2011. Pigments of higher fungi: a review. Czech J Food Sci 29:87–102. https://doi.org/10.17221/524/2010-CJFS.
28. Le Roux A, Meunier S, Le Gall T, Denis JM, Bischoff P, Wagner A. 2011. Synthesis and radioprotective properties of pulvinic acid derivatives. ChemMedChem 6:561–569. https://doi.org/10.1002/cmdc.201000391.
29. Carlsen T, Engh IB, Decock C, Rajchenberg M, Kauserud H. 2011. Multiple cryptic species with divergent substrate affinities in the *Serpula himantioides* species complex. Fungal Biol 115:54–61. https://doi.org/10.1016/j.funbio.2010.10.004.
30. Aqueveque P, Anke T, Sterner O. 2002. The himanimides, new bioactive compounds from *Serpula himantioides* (Fr.) Karst. Z Naturforsch C 57:257–262. https://doi.org/10.1515/znc-2002-3-410.
31. Wang QW, Hidema J, Hikosaka K. 2014. Is UV-Induced DNA damage greater at higher elevation? Am J Bot 101:796–802. https://doi.org/10.3732/ajb.1400010.
32. Smith H, Doyle S, Murphy R. 2015. Filamentous fungi as a source of natural antioxidants. Food Chem 185:389–397. https://doi.org/10.1016/j.foodchem.2015.03.134.
33. Tel G, Ozturk M, Duru ME, Turkoglu A. 2015. Antioxidant and anticholinesterase activities of five wild mushroom species with total bioactive contents. Pharm Biol 53:824–830. https://doi.org/10.3109/13880209.2014.943245.
34. Sindhu ER, Preethi KC, Kuttan R. 2010. Antioxidant activity of carotenoid lutein *in vitro* and *in vivo*. Indian J Exp Biol 48:843–848.
35. Moody SA, Newsham KK, Ayres PG, Paul ND. 1999. Variation in the responses of litter and phylloplane fungi to UV-B radiation (290-315 nm). Mycol Res 103:1469–1477. https://doi.org/10.1017/S0953756299008783.
36. Mustafa U, Kaur G. 2008. UV-B radiation and temperature stress causes variable growth response in *Metarhizium anisopliae* and *Beauveria bassiana* isolates. Internet J Microbiol 7:1–8.
37. Duguay KJ, Klironomos JN. 2000. Direct and indirect effects of enhanced UV-B radiation on the decomposing and competitive abilities of saprobic fungi. Appl Soil Ecol 14:157–164. https://doi.org/10.1016/S0929-1393(00)00049-4.
38. Nematollahi AR, Badiee P, Nournia E. 2015. The efficacy of ultraviolet irradiation on *Trichophyton* species isolated from nails. Jundishapur J Microbiol 8:e18158. https://doi.org/10.5812/jjm.18158v2.
39. Hugues KA, Lawley B, Newsham KK. 2003. Solar UV-B radiations inhibit the growth of Antarctic terrestrial fungi. Appl Environ Microbiol 69:1488–1491. https://doi.org/10.1128/AEM.69.3.1488-1491.2003.
40. Isaac S. 1994. Many fungi are brightly coloured; does pigmentation provide any advantage to those species? Mycologist 8:178–179. https://doi.org/10.1016/S0269-915X(09)80191-2.
41. Zhou ZY, Liu JK. 2010. Pigments of fungi (macromycetes). Nat Prod Rep 27:1531–1570. https://doi.org/10.1039/c004593d.
42. Gill W, Steglich W. 1987. Pigments of fungi (Macromycetes), p 1–297. *In*

Herz W, Grisebach H, Kirby GW, Tamm C (ed), Progress in the chemistry of organic natural products, 1st ed, vol 51. Springer, New York, NY.
43. Moliné M, Libkind D, Diéguez M, van Broock M. 2009. Photoprotective role of carotenoids in yeasts: response to UV-B of pigmented and naturally-occurring albino strains. J Photochem Photobiol B 95:156–161. https://doi.org/10.1016/j.jphotobiol.2009.02.006.
44. Shah F, Mali T, Lundell TK. 2018. Polyporales brown rot species *Fomitopsis pinicola*: enzyme activity profiles, oxalic acid production, and Fe3-reducing metabolite secretion. Appl Environ Microbiol 84:e02662-17. https://doi.org/10.1128/AEM.02662-17.
45. Huang S, Lin C, Mau J, Li Y, Tsai S. 2015. Effect of UV-B irradiation on physiologically active substance content and antioxidant properties of the medicinal caterpillar fungus *Cordyceps militaris* (Ascomycetes). Int J Med Mushrooms 17:241–253. https://doi.org/10.1615/IntJMedMushrooms.v17.i3.40.
46. Purwidyantri A, Rahmandita A, Tsai SY. 2012. Optimization of pulsed UV light irradiation for the production of vitamin D2, bioactive metabolites and antioxidant activity of *Cordyceps militaris* mycelia. Int Proc Chem Biol Environ Eng 39:76–81.
47. Sarikurkcu C, Tepe B, Yamac M. 2008. Evaluation of the antioxidant activity of four edible mushrooms from the Central Anatolia, Eskisehir–Turkey: *Lactarius deterrimus*, *Suillus collitinus*, *Boletus edulis*, *Xerocomus chrysenteron*. Bioresour Technol 99:6651–6655. https://doi.org/10.1016/j.biortech.2007.11.062.
48. Jaworska G, Pogoń K, Skrzypczak A, Bernaś E. 2015. Composition and antioxidant properties of wild mushrooms *Boletus edulis* and *Xerocomus badius* prepared for consumption. J Food Sci Technol 52:7944–7953. https://doi.org/10.1007/s13197-015-1933-x.
49. Kosanić M, Ranković B, Dašić M. 2012. Mushrooms as possible antioxidant and antimicrobial agents. Iran J Pharm Res 11:1095–1102.
50. Vidovic SS, Mujić IO, Zeković ZP, Lepojević ZD, Tumbas VT, Mujić AI. 2010. Antioxidant properties of selected Boletus mushrooms. Food Biophys 5:49–58. https://doi.org/10.1007/s11483-009-9143-6.
51. Tsai SY, Tsai HL, Mau JL. 2007. Antioxidant properties of *Agaricus blazei, Agrocybe cylindracea,* and *Boletus edulis*. Lebenson Wiss Technol 40:1392–1402. https://doi.org/10.1016/j.lwt.2006.10.001.
52. Gao Q, García-Pichel F. 2011. Microbial ultraviolet sunscreens. Nat Rev Microbiol 9:791–802. https://doi.org/10.1038/nrmicro2649.
53. Zou Y, Zhao Y, Hu W. 2015. Chemical composition and radical scavenging activity of melanin from *Auricularia auricula* fruiting bodies. Food Sci Technol (Campinas) 35:253–258. https://doi.org/10.1590/1678-457X.6482.
54. Offord EA, Gautier JC, Avanti O, Scaletta C, Runge F, Krämer K, Applegate LA. 2002. Photoprotective potential of lycopene, carotene, vitamin E, vitamin C and carnosic acid in UVA-irradiated human skin fibroblasts. Free Radic Biol Med 32:1293–1303. https://doi.org/10.1016/S0891-5849(02)00831-6.
55. Varol M, Türk A, Candan M, Tay T, Koparal AT. 2016. Photoprotective activity of vulpinic and gyrophoric acids toward ultraviolet B-induced damage in human keratinocytes. Phytother Res 30:9–15. https://doi.org/10.1002/ptr.5493.
56. Palfner G, Valenzuela-Muñoz V, Gallardo-Escarate C, Parra L, Becerra J, Silva M. 2012. *Cordyceps cuncunae* (Ascomycota, Hypocreales), a new pleoanamorphic species from temperate rainforest in southern Chile. Mycol Prog 11:733–739. https://doi.org/10.1007/s11557-011-0784-8.
57. Doyle JJ. 1990. Isolation of plant DNA from fresh tissue. Focus 12:13–15.
58. White TJ, Bruns TD, Lee SB, Taylor JW. 1990. Amplification and direct sequencing of fungal ribosomal RNA genes for phylogenetics, p 315–322. *In* Innis MA, Gelfand DH, Sninsky JJ, White TJ (eds), PCR protocols: a guide to methods and applications. Academic Press, New York, USA.
59. Altschul SF, Madden TL, Schäffer AA, Zhang J, Zhang Z, Miller W, Lipman DJ. 1997. Gapped BLAST and PSI-BLAST: a new generation of protein database search programs. Nucleic Acids Res 25:3389–3402. https://doi.org/10.1093/nar/25.17.3389.
60. Wu WJ, Ahn BY. 2014. Statistical optimization of ultraviolet irradiate conditions for vitamin D_2 synthesis in oyster mushrooms (*Pleurotus ostreatus*) using response surface methodology. PLoS One 9:e95359. https://doi.org/10.1371/journal.pone.0095359.
61. Trest M, Will-Wolf S, Keuler R, Shay N, Hill K, Studer A, Muench A, Alexander Z, Adams A, Dittberner L, Feehan M, Lee H, Galleguillos-Katz N, Zedler J, Graham L, Arancibia-Avila P. 2015. Potential impacts of UV exposure on lichen communities: a pilot study of *Nothofagus dombeyi* trunks in southernmost Chile. Ecosyst Health Sustain 1:1–12. https://doi.org/10.1890/EHS15-0008R1.1.
62. Rain-Franco A, Muñoz C, Fernandez C. 2014. Ammonium production of central Chile (36°S) by photodegradation of phytoplankton-derived and marine dissolved organic matter. PLoS One 9:e100224. https://doi.org/10.1371/journal.pone.0100224.
63. López SN, Greslebin AG, González SB, Pildain MB. 2013. Effect of water potential and host defense on the growth of *Amylostereum areolatum* and *A. chailletii*, fungal symbionts of siricides, and study of wood associated mycobiota of conifers in Patagonia, Argentina. Bosque (Valdivia) 34:161–171.
64. Pereira G, Herrera J, Machuca A, Sánchez M. 2007. Effect of pH on the *in vitro* growth of ectomycorrhizal fungi collected from *Pinus radiata* plantations. Bosque (Valdivia) 28:215–219.
65. El-Gali Z. 2015. Antagonism capability in vitro of *Trichoderma harzianum* against *Alternaria alternata* on *Ceratonia siliqua*. Eur J Pharm Med Res 2:30–44.
66. Zacchi L, Morris I, Harvey PJ. 2000. Disordered ultrastructure in lignin-peroxidase secreting hyphae of the white-rot fungus *Phanerochaete chrysosporium*. Microbiology 146:759–765. https://doi.org/10.1099/00221287-146-3-759.
67. Huang YT, Onose J, Abe N, Yoshikawa K. 2009. In vitro inhibitory effects of pulvinic acid derivates isolated from Chinese edible mushrooms, *Boletus calopus* and *Suillus bovinus*, on cytochrome P450 activity. Biosci Biotechnol Biochem 73:855–860. https://doi.org/10.1271/bbb.80759.
68. Umashankar T, Govindappa M, Ramachandra YL. 2014. *In vitro* antioxidant and antimicrobial activity of partially purified coumarins from fungal endophytes of *Crotalaria pallida*. Int J Curr Microbiol Appl Sci 3:58–72.
69. Scott JW, Cort WM, Harley H, Parrish DR, Saucy G. 1974. 6-Hydroxychroman-2-carboxylic acids: novel antioxidants. J Am Oil Chem Soc 51:200–203. https://doi.org/10.1007/BF02632894.
70. Dong JW, Cai L, Xing Y, Yu J, Ding ZT. 2015. Re-evaluation of ABTS*+ assay for total antioxidant capacity of natural products. Nat Prod Commun 10:2169–2172.
71. Sugiharto S, Yudiarti T, Isroli I. 2016. Assay of antioxidant potential of two filamentous fungi isolated from the Indonesian fermented dried cassava. Antioxidants (Basel) 5:6. https://doi.org/10.3390/antiox5010006.
72. Ou B, Chang T, Huang D, Prior RL. 2013. Determination of total antioxidant capacity by oxygen radical absorbance capacity (ORAC) using fluorescein as the fluorescence probe: First Action 2012.23. J AOAC Int 96:1372–1376. https://doi.org/10.5740/jaoacint.13-175.
73. Prior RL, Wu X, Schaich K. 2005. Standardized methods for the determination of antioxidant capacity and phenolics in foods and dietary supplements. J Agric Food Chem 53:4290–4302. https://doi.org/10.1021/jf0502698.
74. Caddeo C, Teskac K, Sinico C, Kristl J. 2008. Effect of resveratrol incorporated in liposomes on proliferation and UV-B protection of cells. Int J Pharm 363:183–191. https://doi.org/10.1016/j.ijpharm.2008.07.024.
75. Mosmann T. 1983. Rapid colorimetric assay for cellular growth and survival: application to proliferation and cytotoxicity assays. J Immunol Methods 65:55–63. https://doi.org/10.1016/0022-1759(83)90303-4.